

RESEARCH

Open Access



# Enhancing *Akkermansia* growth via phytohormones: a strategy to modulate the gut-bone axis in postmenopausal osteoporosis therapy

Zhiqi Zhao<sup>1,2</sup> , Yixuan Deng<sup>3</sup>, Li Li<sup>4</sup>, Liying Zhu<sup>1</sup>, Xin Wang<sup>1</sup>, Haibiao Sun<sup>2</sup>, Xiaoqiong Li<sup>1\*</sup>, Xiaoqiang Han<sup>2\*</sup> and Jinjun Li<sup>1\*</sup>

## Abstract

**Background** Phytohormones have garnered considerable interest as potential modulators of the gut-bone axis. Denosumab (Deno), a widely utilized therapeutic agent for postmenopausal osteoporosis, has not been previously investigated for its effects on gut health. The objective of this study was to assess the efficacy of isoflavones (SI), naringin (Nar), and Deno in the management of postmenopausal osteoporosis by targeting the gut-bone axis.

**Methods** The postmenopausal osteoporosis model in mice was established via bilateral oophorectomy. Subsequently, mice in the Deno group received subcutaneous injections of Deno at a dosage of 10 mg/kg, administered twice weekly. In contrast, mice in the SI and Nar groups were subjected to oral gavage with 200 mg/kg/day of SI and Nar, respectively. The treatment period for all groups lasted for 8 weeks. Upon the conclusion of the experiment, a thorough evaluation of the effects of SI, Nar, and Deno on bone and gut health in mice was conducted through immunological, pathological, imaging, and multi-omics methodologies.

**Results** Deno, SI, and Nar significantly alleviated the physical symptoms in postmenopausal mice. However, only SI and Nar significantly modulated the gut microbiota. *Akkermansia* was significantly enriched after the gavage of SI and Nar. *Akkermansia* has the capacity to not only augment bone mass and alleviate strength deterioration via extracellular vesicles, but it also influences bone metabolism by diminishing inflammation and modulating lipid metabolism. Notably, no significant changes in the gut microbiota were observed in the Deno group, which may be attributed to the differences in the method of administration, as Deno was administered via subcutaneous injection rather than gavage.

**Conclusion** SI and Nar may influence the gut-bone axis through *Akkermansia* and have the potential of alternative treatment options for postmenopausal osteoporosis. Although the gut microbiota is not significantly affected by the subcutaneous administration of Deno, the long-term management of postmenopausal osteoporosis and the exploration of various management models warrant additional scrutiny. Furthermore, this study has yet to

\*Correspondence:

Xiaoqiong Li  
0707lianlan@163.com  
Xiaoqiang Han  
jack98193@163.com  
Jinjun Li  
lijinjun@zaas.ac.cn

Full list of author information is available at the end of the article

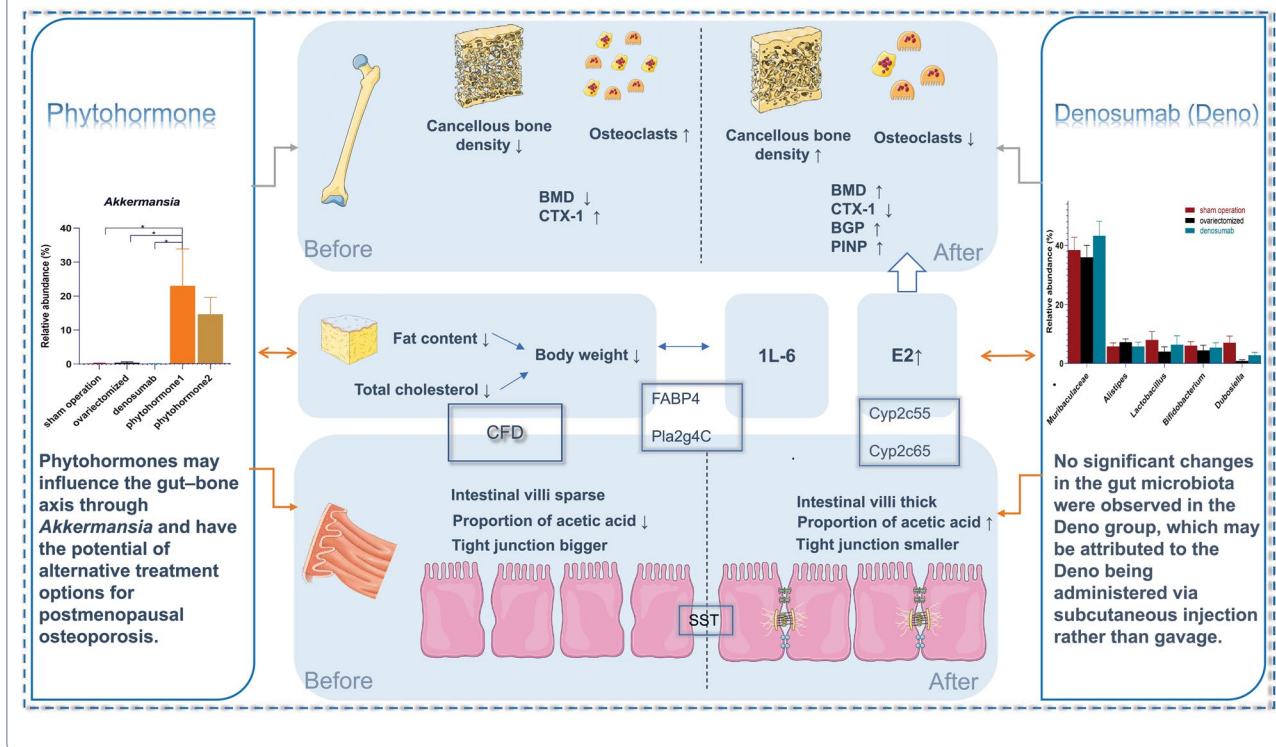


© The Author(s) 2025. **Open Access** This article is licensed under a Creative Commons Attribution-NonCommercial-NoDerivatives 4.0 International License, which permits any non-commercial use, sharing, distribution and reproduction in any medium or format, as long as you give appropriate credit to the original author(s) and the source, provide a link to the Creative Commons licence, and indicate if you modified the licensed material. You do not have permission under this licence to share adapted material derived from this article or parts of it. The images or other third party material in this article are included in the article's Creative Commons licence, unless indicated otherwise in a credit line to the material. If material is not included in the article's Creative Commons licence and your intended use is not permitted by statutory regulation or exceeds the permitted use, you will need to obtain permission directly from the copyright holder. To view a copy of this licence, visit <http://creativecommons.org/licenses/by-nc-nd/4.0/>.

establish a dose–response relationship, indicating that further research is essential to clarify the regulatory effects of varying doses of SI and Nar on postmenopausal osteoporosis especially the modulation of gut microbiota.

**Keywords** Osteoporosis, Phytohormones, Soybean isoflavone, Naringin, Denosumab, Gut microbiome

**Graphical Abstract**



**Introduction**

Osteoporosis is a widespread bone disease primarily attributed to estrogen deficiency, characterized by reduced bone mass and the deterioration of bone ultrastructure, resulting in bone fragility [1]. This condition is a major risk factor for fractures in women over the age of 50 [2, 3]. Postmenopausal bone loss arises from an imbalance between bone formation and resorption, driven by increased bone remodeling activity [4]. Additionally, postmenopausal obesity as well as the increase in autoimmune diseases can also increase the risk of developing osteoporosis [5]. Estrogen therapy is commonly prescribed for the treatment and prevention of osteoporosis. However, given the potential adverse effects associated with long-term estrogen supplementation, there is a concerted effort to explore and develop phytohormones as alternative therapeutic options [2].

Phytohormones can interact with microbes acting as estrogen agonists to prevent bone loss after menopause

[6, 7]. In particular, flavonoids have shown great potential in treating postmenopausal osteoporosis [8, 9]. Moreover, soy products and supplements enriched with isoflavones have gained popularity as substitutes for estrogen replacement therapy [10]. Consistent consumption of soy isoflavones, a type of flavonoid compound, has been shown to reduce conditions influenced by estrogen levels and can partially mitigate the onset of osteoporosis in postmenopausal women [11, 12]. Furthermore, daily supplementation with soy protein has been demonstrated to positively influence bone metabolism [13]. Naringin (Nar), another flavonoid with estrogenic properties, has been studied for its effects on bone health [14]. Specifically, Nar supplementation in ovariectomized rats with osteoporosis has been demonstrated to enhance bone metabolism and improve the structures of cortical bone and bone trabecula [15]. In postmenopausal women, the consumption of Nar can significantly improve arterial stiffness [16]. Additionally, Nar has been shown to improve blood lipid status in

patients with obesity and exhibit therapeutic effects against bronchopneumonia [17].

The gut–bone relationship is receiving increasing attention in the field of skeletal wellness. The gut microbiota has the capacity to affect bone homeostasis by altering host metabolism, immune responses, and hormone production [18]. Notably, alterations in the gut microbiome have been associated with reductions in both bone density and mass [19], with a marked decrease in bone mineral content observed following total gastrectomy [20]. Furthermore, dysbiosis of the gut microbiota impairs the intestinal absorption of calcium, which in turn influences osteoclast activity and bone structure [21].

Dietary supplements have the potential to influence the balance of gut microecology [22]. Certain phytohormones have been shown to exert remarkable estrogenic effects through their interactions with gut microbiota [23–26]. Previous studies indicate that ICR mice are often used to develop the mouse model for postmenopausal osteoporosis [27–29]. Additionally, it has been reported that SI and Nar play a role in regulating gut microbiota, safeguarding the intestinal tract, and enhancing host health [23–26]. Denosumab (Deno), an anti-RANKL monoclonal antibody, is an effective treatment for postmenopausal osteoporosis, as it inhibits the development and activity of osteoclasts while promoting increased bone density [3]. However, the effects of Deno on the gut microbiota in osteoporotic mice remain to be investigated. Therefore, the primary aim of the present study is to compare the effects of SI and Nar with those of Deno on postmenopausal ICR mice with osteoporosis and elucidate the mechanism associated with the bone–intestinal axis effect.

## Methods

### Animals and reagents

Thirty-five female mice, aged 8 weeks, were obtained from Shanghai Slack Laboratory Animal Co., Ltd. These mice were specific pathogen-free (SPF) and belonged to the Institute of Cancer Research (ICR) strain [28]. SI (CAS:574-12-9) and Nar (CAS: 67604-48-2) were purchased from Aladdin. Enzyme-linked immunosorbent assay (ELISA) kits used to detect the serum levels of estradiol (E2), interleukin-6 (IL-6), type I collagen C-terminal peptide (CTX-1), propeptide of type I procollagen (PINP), and bone gla-containing protein (BGP) were purchased from Nanjing Jiancheng Co., Ltd.

### Experimental animal model construction

The mice were anesthetized with 3% isoflurane, followed by disinfection of their skin with 10% povidone iodine. Two incisions were subsequently

made, penetrating both the skin and musculature of the dorsal region. Subsequently, 28 mice were sutured after bilateral oophorectomy, while 7 mice were designated as the sham operation (SO) group ( $n=7$ ) and were sutured without oophorectomy. Postoperatively, all mice received intramuscular injections of 50,000 U/D penicillin for a duration of three days. Twenty-eight days following the surgery, the ovariectomized mice were divided into four distinct groups: the ovariectomized (OVX) group ( $n=7$ ), the denosumab treatment (Deno) group ( $n=7$ ), the soy isoflavone (SI) treatment group ( $n=7$ ), and the naringenin (Nar) treatment group ( $n=7$ ). Mice recovered within 13 weeks after surgery, during which they had unrestricted access to food and water. By the end of the 13th week, administration of Deno, genistein, and hesperidin commenced. Deno, a widely utilized clinical medication, was administered at a dosage of 60 mg biannually. The equivalent dosage for mice was calculated based on body surface area, resulting in a dosage of 20.13699 mg/kg. Additionally, in accordance with previous literature [4], a subcutaneous dosage of 10 mg/kg was administered twice weekly to the Deno group. For the SI and Nar groups, the effective and safe dosages of soy isoflavone and naringenin were identified to range from 75 to 300 mg/kg/d, demonstrating a dose-dependent effect. Based on prior research conducted in our laboratory on flavonoid compounds, a dosage of 200 mg/kg/d was selected for oral gavage (dissolved in 1 ml physiological saline). All treatments last for 8 weeks. During the experiment, the mice were provided unrestricted access to food and sterile water. The mice were provided with standard maintenance feed from Jiangsu Xietong Biological Co., Ltd. The SPF-rated animal facility was maintained at a temperature range of 22–24 °C and a humidity level of 50–60%.

### Sample collection

After eight weeks of intervention, the mice were anesthetized using 3% isoflurane, after which blood samples were collected from the abdominal aorta. Prior to anesthesia, the body weight of the mice was recorded, and subsequent to the excision, the weights of the liver, spleen, and adipose tissue were measured. The lengths of the colon, cecum, ileum, and jejunum were documented. The ileal segment was preserved in a solution suitable for electron microscopy, while the colon and its contents were stored at  $-80$  °C. Both femurs from each mouse were immersed in 4% paraformaldehyde and maintained at 4 °C. Fecal samples were collected from the mice the day before euthanasia and were also preserved at  $-80$  °C.

### Preparation of bone imaging indices and pathological sections

A small animal dual energy instrument (iNSiGHT VET DXA, OsteoSys, Korea) was used to measure the bone mineral density (BMD) of the right femur through in vivo computed tomography (CT) imaging of the small animal. The left femur samples were preserved in 4% paraformaldehyde fixative (Wuhan Seville Biotechnology Co., Ltd., Wuhan, China). Following preservation, the tissue was trimmed, dehydrated, nested, and sliced two days later. Sections of bone tissue were subjected to hematoxylin and TRAP (tartrate-resistant acid phosphatase) staining techniques (Wuhan Seville Biotechnology Co., Ltd., Wuhan, China) and then imprinted with neutral resin (Wuhan Seville Biotechnology Co., Ltd.). Microscopy images were captured using a microscope (Nikon Eclipse C1, Nikon Limited) at a magnification of 200×. The quantification of osteoclasts within each section was conducted with Image 6.0.

### Determination of blood indices

Serum levels of E2, IL-6, CTX-1, BGP, and PINP levels were measured using ELISA kits. Blood concentrations of total cholesterol (CHO), triglyceride (TG), low-density lipoprotein (LDL), high-density lipoprotein (HDL), and other biochemical indicators were detected with an automatic biochemical instrument from Wuhan Xeville Company (Chemray240, Wuhan, China).

### Identification of metabolites within intestinal contents

The GC-2010 Plus gas chromatograph (Shimadzu Corporation, Kyoto, Japan) was utilized to quantify the short-chain fatty acids (SCFAs) in the colonic contents of the mice, following a methodology previously established [30]. In brief, a 10% fecal homogenate was prepared and subjected to centrifugation, after which the supernatant was collected and filtered. The filtrate was subsequently acidified at  $-80^{\circ}\text{C}$  for 24 h. The content of acetic acid, propionic acid, butyric acid, valeric acid, isobutyric acid, and isovaleric acid in the feces samples were then analyzed.

### Intestinal ultrastructure analysis

Tissue blocks, each with a volume of  $1\text{ mm}^3$ , were excised from the ileum of each mouse and immersed in a fixation solution suitable for electron microscopy, contained within an EP tube. This solution consisted of 2.5% glutaraldehyde dissolved in 0.1 M phosphate buffer. Post fixation, the tissues were embedded in paraffin and sectioned using a microtome. Images were then acquired using an HT7800 transmission electron microscope

(manufactured by HITACHI, Japan) at magnification of  $\times 700$  and  $\times 1500$ .

### 16S rRNA sequencing and transcriptome sequencing

The microbial composition of mouse feces was analyzed by Lianchuan Biological Co., Ltd. (Hangzhou, Zhejiang). Genomic DNA was extracted from cecal fecal samples using the QIAamp DNA Fecal Mini Kit (Qiagen 51504) and subsequently sequenced. The V3-V4 hypervariable region of the 16S rDNA gene was amplified through PCR utilizing the primers 341F: 5'-CCTACGGGNGGCWGCAG-3' and 806R: 5'-GGACTACHVGGGTATCTAAT-3', with each sample assigned a unique eight-base barcode. The obtained amplicon was excised from the 2% agarose gel and subsequently purified following the protocol of the AxyPrep DNA Gel Extraction Kit (Axygen Biosciences, USA) in accordance with the kit's protocol. The quantity of the purified amplicon was then assessed using the Quantifluoro-st reagent (Promega, USA). The amplified DNA fragment, after purification, underwent equimolar clustering and was sequenced on both ends using a  $2\times 250$  bp protocol on the Illumina sequencing system, adhering to the established standard procedures.

The colons of the mice were excised and preserved at  $-80^{\circ}\text{C}$  for the purpose of total RNA extraction, following the protocols outlined in the RNA sample preparation kit (Illumina, San Diego, CA, USA). The integrity and total quantity of the RNA were assessed using bioanalyzers. Subsequently, RNA sequencing was conducted by Mingke Biotechnology Co., Ltd. (Hangzhou, China).

### Data analysis

Statistical analyses were performed utilizing GraphPad 8.0, and the data are presented as the means  $\pm$  standard deviation (SD). The Shapiro–Wilk test and Levene's test for normality and homogeneity of variance were conducted using the R package 'car'. More than 85% of the datasets adhered to the criteria for normal distribution and met the assumption of homogeneity of variance. In recognition of the inherent biological variability in experimental studies, all data points were retained, including outliers, to provide a complete representation of findings. For the statistical analysis, one-way ANOVA was selected to evaluate the significance of differences among treatment groups. Subsequent to identifying significant differences, the Student–Newman–Keuls post-hoc test was performed to facilitate pairwise comparisons between each group. The Spearman correlation coefficient was used for correlation analysis. The bacterial diversity and species composition results were analyzed using Qiime2 and R 4.2.1.  $P < 0.05$  was considered statistically significant.

**Results**

**Impact of phytohormones and denosumab on bone improvement and body weight in ovariectomized mice**

CT imaging of the bone microarchitecture demonstrated a significant reduction in cancellous bone density in the OVX group compared to the SO group. In contrast, the cancellous bone in the Deno, SI, and Nar groups exhibited a more compact structure (Fig. 1Aa). The

BMD in the OVX group was notably lower than that in the SO group ( $P < 0.0001$ , Fig. 1Aa, Ab, and B), whereas the BMD in the Deno, SI, and Nar groups was notably greater than that in the OVX group ( $P < 0.0001$ ). Besides, using the R packages lsr and pwr, the effect size for the BMD indicators was calculated, and a power analysis yielded a value of 0.828, indicating that the sample size in each group is sufficient to support the reliability of

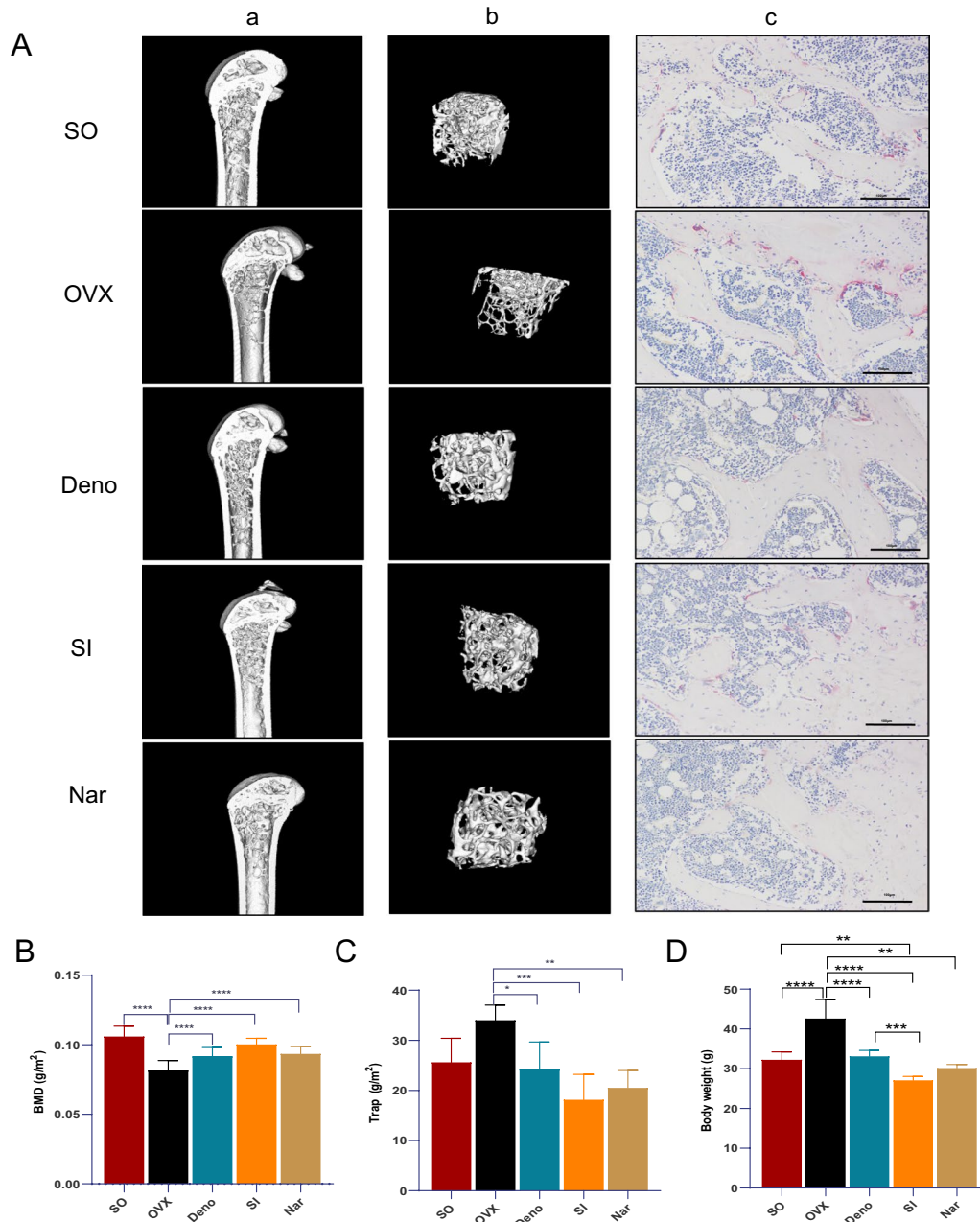


**Fig. 1** CT images of the distal femoral region (Aa) and the cancellous bone at the distal end of the femur (Ab) of mice from each group and images of pathological sections (Ac). **B** Bone mineral density (BMD) measurements. **C** Osteoclast number. **D** Body weight. All the data are expressed as the means  $\pm$  SD.  $n = 5-7$ , \* $P < 0.05$ , \*\* $P < 0.01$ , \*\*\* $P < 0.001$ , and \*\*\*\* $P < 0.0001$

the results. Moreover, mice in the OVX group exhibited a significantly higher number of osteoclasts and greater body weights compared to those in the SO group ( $P < 0.05$ ,  $P < 0.0001$ ; Fig. 1Ac, C, and D), whereas those in the Deno, SI and Nar groups displayed a significantly lower number of osteoclasts and body weights compared to the OVX group did ( $P < 0.01$ ; Fig. 1D).

However, no significant differences were observed in the liver indices, spleen indices, and overall fat content among the various groups. It is important to highlight that the fat index in the SI group exhibited a marked reduction in comparison to the other four groups ( $P < 0.01$ ; Fig. S1).

The results of this study demonstrate that treatment with SI, Nar, or Deno resulted in a significant increase in BMD, alongside a reduction in body weight and osteoclast count in ovariectomized mice. Besides, when compared to Deno, both SI and Nar exhibited more pronounced effects on BMD, osteoclast count, body weight, and fat index, with the SI group showing particularly notable improvements.

#### Effects of phytohormones and denosumab on the blood indices of ovariectomized mice

Based on well-established imaging techniques, identified pathologies, and blood markers of bone metabolism [31, 32]. The results of the ELISA revealed a significant reduction in serum estradiol (E2) levels in the ovariectomized (OVX) group compared to the SO group ( $P < 0.0001$ , Fig. 2A). Furthermore, the concentrations of BGP and PINP were decreased, although these changes were not statistically significant (Fig. 2D, E). Treatment with Deno, SI, and Nar resulted in increased levels of E2, BGP, and PINP. Additionally, the serum concentration of CTX-1 was significantly enriched in the OVX group compared with the SO group ( $P < 0.05$ , Fig. 2C), while it was significantly reduced in the Deno, SI, and Nar groups relative to the OVX group ( $P < 0.01$ ). Moreover, although the IL-6 levels were higher in the OVX group compared to the other groups, this difference did not reach statistical significance.

In comparison to the SO group, the levels of CHO, TG, and LDL level in blood were significantly increased ( $P < 0.05$ , Fig. 2F, G, and H). Conversely, the Deno and Nar groups exhibited a significant reduction solely in cholesterol levels, while the SI group demonstrated a significant decrease in both cholesterol and triglyceride levels. Notably, there was no significant difference in HDL between the OVX group and other groups.

Collectively, these results suggest that SI, Nar, and Deno markedly elevated the levels of E2, BGP, and PINP in ovariectomized mice, while concurrently reducing the concentrations of CTX-1 and CHO content. In particular,

the SI group also demonstrated a significant reduction in triglyceride levels.

#### Effects of phytohormones and denosumab on SCFAs

The composition of the intestinal metabolites in each experimental group was illustrated in Fig. 3A, with acetic acid constituting the predominant component in all groups. The total acid content did not significantly differ among the groups (Fig. S2). Compared to the SO group, the Deno group had no significant effect on the levels of acetic acid and propionic acid in the intestinal tract of mice (Fig. 3B, C). Interestingly, compared with the SO and OVX groups, the proportion of acetic acid increased significantly after treatment with Deno or SI ( $P < 0.05$ ), while the proportion of propionic acid was significantly reduced ( $P < 0.05$ ). However, the significantly reduced isovaleric acid content in the OVX group did not recover following any treatment ( $P < 0.05$ ; Fig. 3D). Additionally, the proportions of isobutyric acid and valeric acid in the OVX group have no significant difference with any other group (Fig. 3E, F). Besides, the treatment of Deno, SI and Nar all restore the significant increase of butyric acid in the OVX group ( $P < 0.05$ ; Fig. 3G).

Hence, SI, Nar, and Deno each increased the proportion of acetic acid, decreased the level of propionic acid, and reinstated the significant increase of butyric acid in the OVX group.

#### Effects of phytohormones and denosumab on intestinal microbial

The rarefaction curves demonstrated that both the sequencing depth and uniformity were sufficient (Fig. S3). The Chao1 index and Shannon index did not significantly differ among the groups (Fig. 4A, C). In contrast, the Simpson index in the SI group was significantly lower than that in the SO, OVX, and Deno groups ( $P < 0.05$ , Fig. 4B). There were significant differences in the composition of intestinal flora among the groups (Fig. 4D, E, Fig. S4A). Furthermore, ANOSIM analysis showed significant differences between the SI or Nar groups and the OVX and SO groups ( $P = 0.001$ ; Fig. S4B–D). At the genus level, 103 operational taxonomic units (OTUs) were found to coexist, with the diversity of the Nar group being distinctly different from that of the other groups (Fig. S4E). Consequently, the Nar exhibited a more pronounced impact on bacterial abundance and diversity, displaying a species distribution similar to that of the SI group. Moreover, Deno did not significantly alter bacterial diversity. The composition of phylum and genus in each group is shown in Fig. 4F and G, respectively. At the phylum level, the abundance of Verrucomicrobia in the SI and Nar groups was

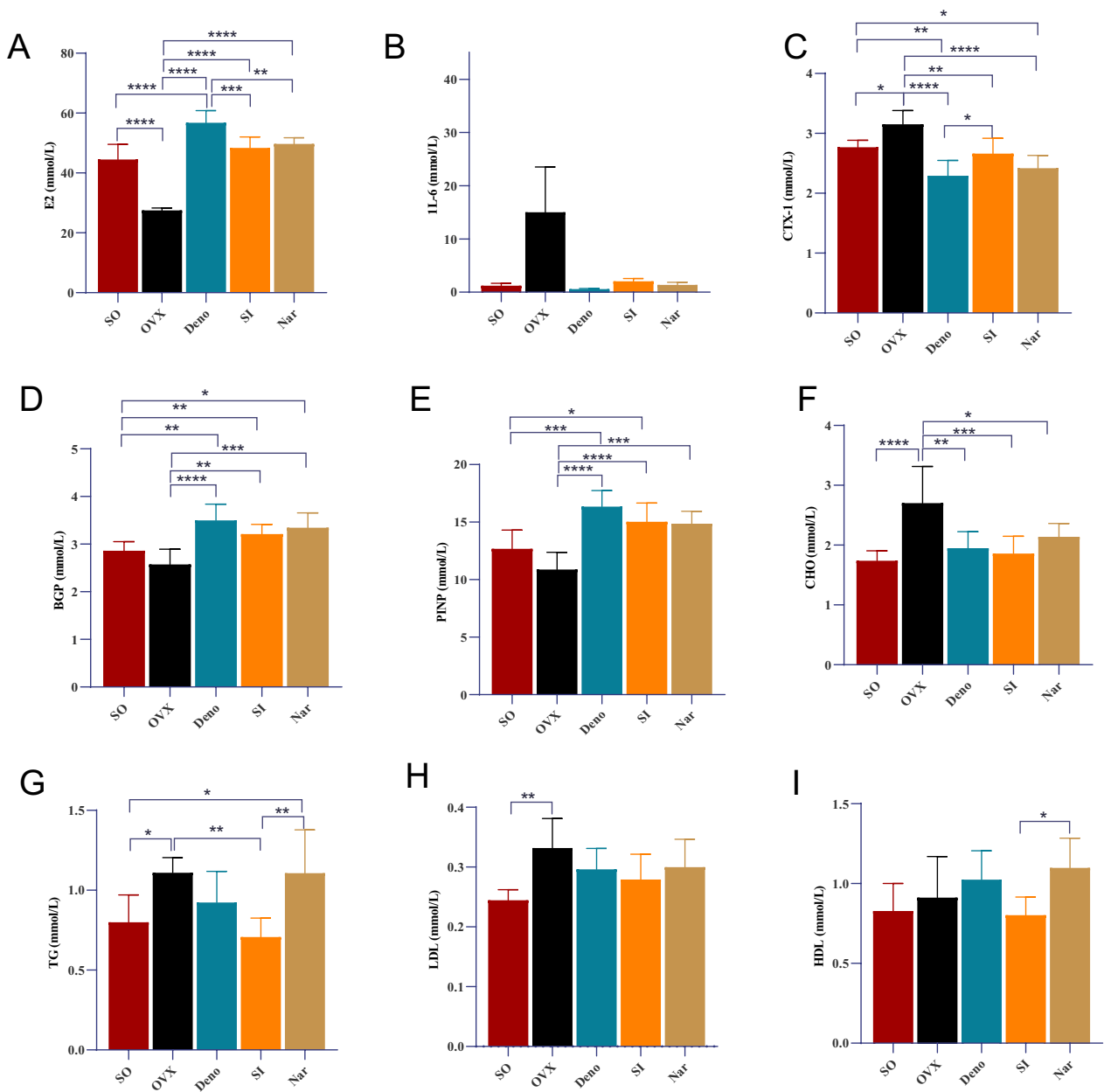


**Fig. 2** Blood indicators associated with osteoporosis. **A** Estradiol (E2); **B** Interleukin 6 (IL-6); **C** C-terminal peptide of type I collagen (CTX-1); **D** Osteocalcin (BGP); **E** Propeptide of type I procollagen (PINP); **F** Total cholesterol (CHO); **G** Triglyceride (TG); **H** Low-density lipoprotein (LDL); **I** High-density lipoprotein (HDL). All data are expressed as mean  $\pm$  SD. n = 7, \* $P < 0.05$ , \*\* $P < 0.01$ , \*\*\* $P < 0.001$ , and \*\*\*\* $P < 0.0001$

increased, while the abundance of Bacteroidetes decreased relative to that in the other groups (Fig. 4F). At the genus level, SI and Nar groups significantly enhanced the abundance of *Akkermansia* ( $P < 0.05$ ; Fig. S5). Moreover, *Akkermansia* was identified as the most critical genus on the basis of the random forest analysis ( $P < 0.05$ ; Fig. S4F).

#### Differences of phytohormones and denosumab on the intestinal bacterial composition

The representative flora for each group were determined using a cutoff of  $LDA > 3$ ,  $P < 0.05$  cutoff (Fig. 5A-B, S6). Compared with the SO group, the OVX group decreased *Dubosiella*, *Parasutterella*, *millionella*, *DTU014\_unclassified*, *Defluviitaleaceae\_UCG\_011*,

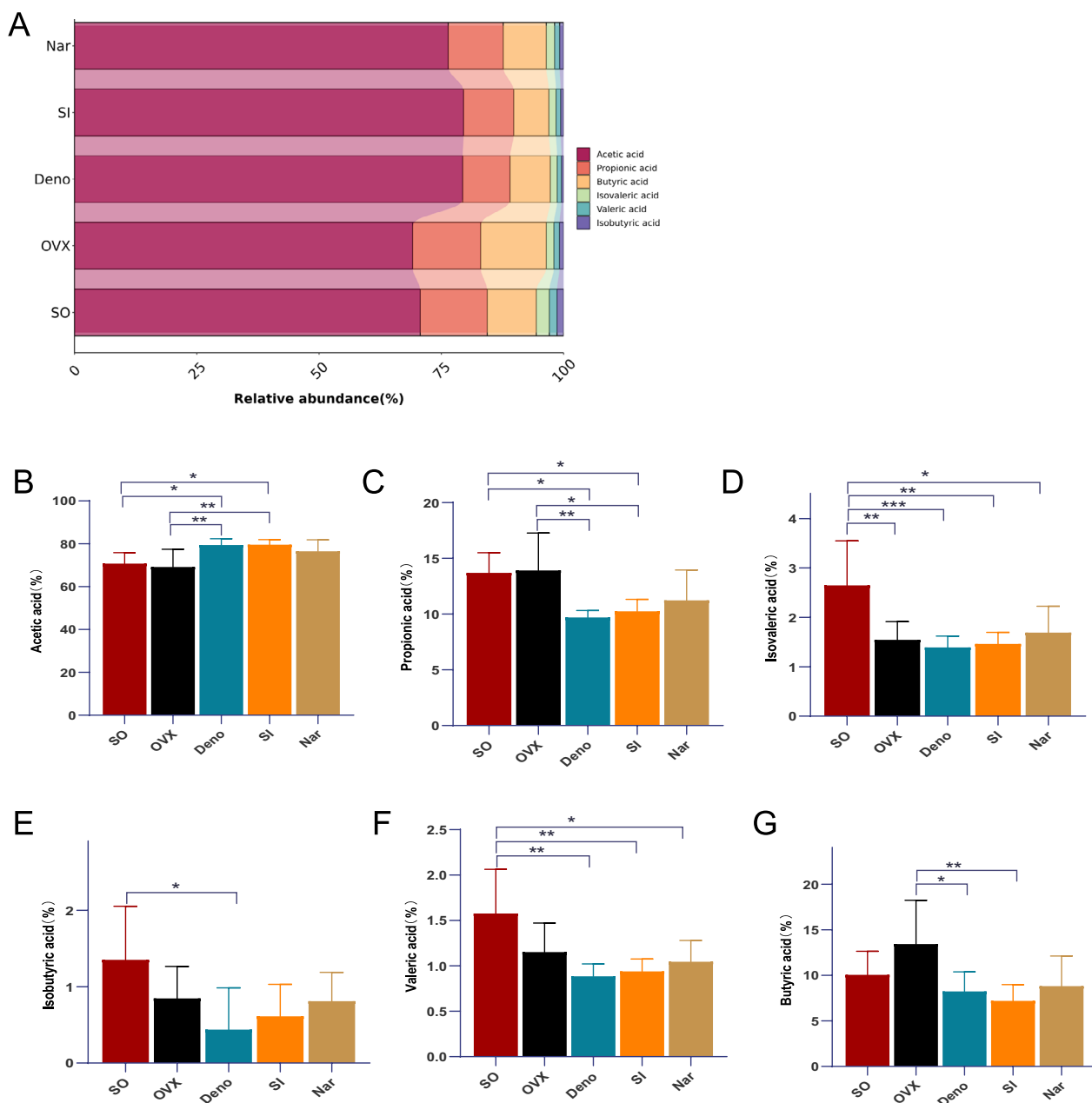


**Fig. 3** Changes in intestinal metabolites. **A** Composition of short-chain fatty acids; **B** Acetic acid content; **C** Propionic acid content; **D** Butyric acid content; **E** Valeric acid content; **F** Isobutyric acid content; **G** Isovaleric acid content. All the data are expressed as mean  $\pm$  SD.  $n = 7$ ,  $*P < 0.05$ ,  $**P < 0.01$ ,  $***P < 0.001$ , and  $****P < 0.0001$

and *Christensenellaceae\_R\_7\_group*, and significantly increased *Robinsoniella*, *Desulfovibrionaceae\_unclassified*, *Gastranaerophilales\_unclassified*, *GCA\_900066575*, *Clostridium*, *Odoribacter*, *Helicobacter*, *Rikenella*, *Ruminococcaceae\_UCG\_014*, *Clostridiales*. Treat with Deno reduced *Absiella* and *Alloprevotella*. SI and Nar both increased *Akkermansia*, and *Clostridium\_sensu\_stricto\_1*, decreased *Absiella*,

*Bacteroides*, and *Parabacteroides* in OVX mice, while SI also increased *Candidatus\_Saccharimonas*, decreased *Aneroplasma*, *Peptococcaceae\_unclassified*, *GCA\_900066575*, *Ruminiclostridium\_5*, *Negativibacillus*, *Eubacterium\_nodatum\_group*, *Candidatus\_Arthromitus*, *Marvinbryantia*, *Anaerovorax*, *Acidiferrobacteraceae\_unclassified*, and *Lactobacillus*, and Nar also increased *Ruminiclostridium\_9*, *Ruminiclostridium*,

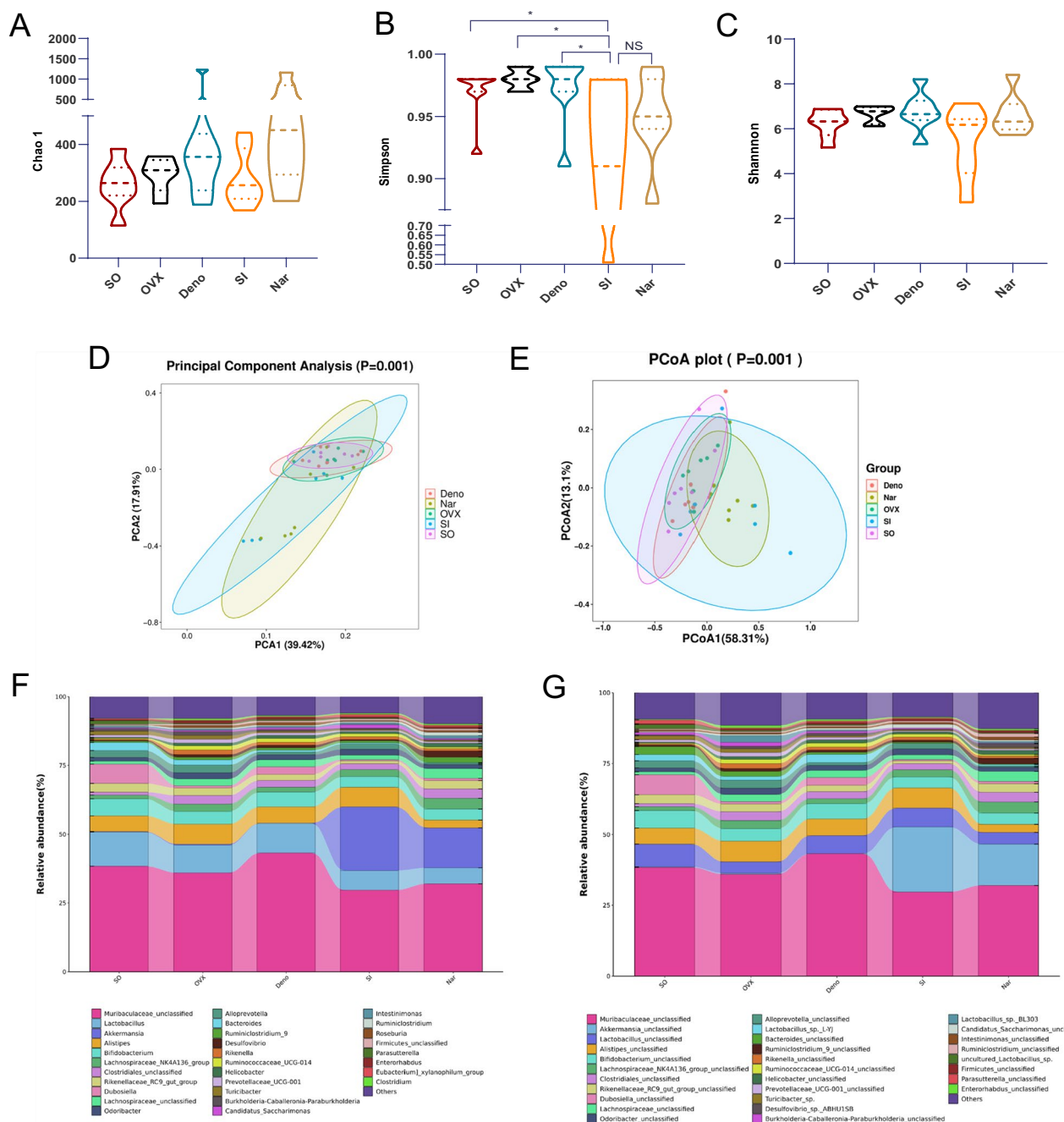


**Fig. 4** Diversity and composition of intestinal microbiota in ovariectomized mice. **A** Chao1 index; **B** Shannon index; **C** Simpson index; **D** Principal coordinate analysis (PCA). **E** Principal coordinate analysis (PCoA); **F** Bacterial composition at the phylum level; **G** Bacterial composition at the genus level. All data were mapped and analyzed using QIIME2, and R 4.2.1.  $n = 7$ , \* $P < 0.05$ , \*\* $P < 0.01$ , \*\*\* $P < 0.001$ , and \*\*\*\* $P < 0.0001$

*Intestinimonas*, *Acetatifactor*, *Oscillibacter*, *Anaerovorax*, *Oscillospira*, *Kineothrix*, *Eubacterium\_oxidoreducens\_group*, *Family\_XIII\_UCG\_001*, *Ruminococcaceae\_UCG\_010*, and *Bilophila*, decreased *Sphingopyxis*, *Ruminococcaceae\_UCG\_014*, *Alloprevotella*, and *Alistipes*.

**Indicated flora analysis and correlation**

**between the intestinal flora and osteoporosis phenotype**

Correlation analysis between bone markers and other disease phenotypes (Fig. 6D) revealed that body weight and TG, CHO, LDL, and HDL levels were significantly negatively correlated with BMD ( $P < 0.05$ ). The serum E2

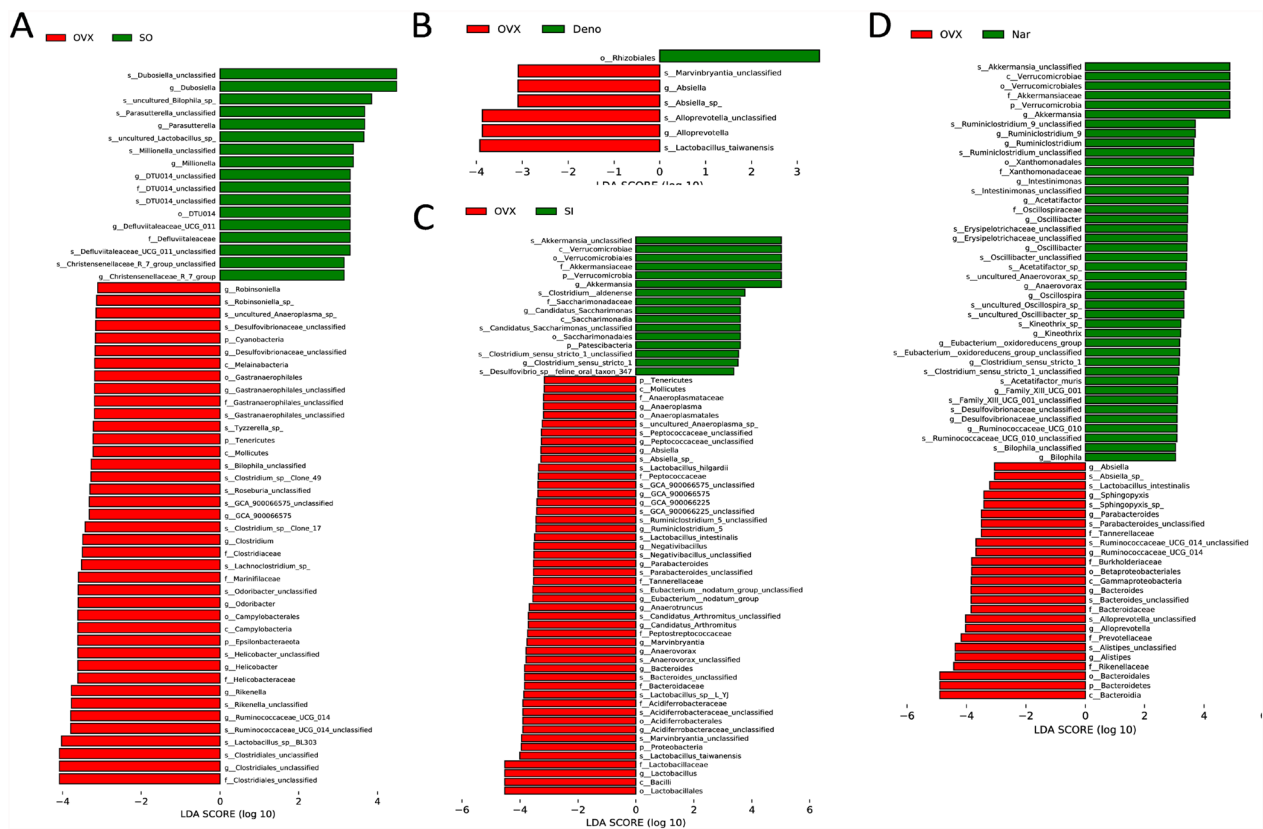


**Fig. 5** Clodogram and Linear Discriminant Analysis (LDA) score of the statistically significant microbial groups in the four groups (A–D). All data were mapped and analyzed using R 4.2.1.  $n = 7$ . **A**—OVX (Ovariectomy) vs. SO (Sham Operation); **B**—Deno (Denosumab) vs. OVX; **C**—SI (Isoflavone) vs. OVX; **D**—Nar (Naringin) vs. OVX

content was negatively correlated with CTX-1 ( $P < 0.01$ ). Serum PINP was positively correlated with E2 ( $P < 0.05$ ), whereas HDL was negatively correlated with IL-6 and body weight. Moreover, the serum BGP was positively correlated with E2 ( $P < 0.05$ ), and HDL was negatively correlated with body weight ( $P < 0.05$ ). Hence, improved lipid metabolism and body weight might have promoted increased BMD, whereas improved E2 levels might reduce CTX-1 abundance and increase the PINP and BGP contents. Additionally, a decrease in IL-6 might promote an increase in PINP.

We conducted a comparative analysis of the aforementioned phenotypic outcomes in relation to the intestinal microbiota and  $\alpha$  diversity. Our findings indicated a significant negative correlation between mouse body weight and the presence of *Akkermansia* ( $P < 0.05$ ; Fig. 6E), while a significant positive correlation was observed between *Akkermansia* and the Simpson index ( $P < 0.05$ ). Additionally, BMD was positively correlated with *Akkermansia* ( $P < 0.1$ ), whereas CTX-1 was negatively correlated with *Alistipes* ( $P < 0.05$ ) (Fig. 6F). Furthermore, redundancy analysis (RDA)

results further revealed that BMD, BGP, PINP, and *Akkermansia* were positively correlated, whereas body weight and the levels of CTX-1, E2, and *Akkermansia* were negatively correlated (Fig. 6G).

### Effects of phytohormones and denosumab on gene expression

In the OVX group, 283 genes were upregulated and 170 were downregulated compared with the SO group (Fig. S7A). In contrast, the Deno group showed an upregulation of 171 genes and a downregulation of 125 genes relative to the OVX group (Fig. S7B). The SI group displayed an equal number of upregulated and downregulated genes, with 54 genes in each category (Fig. S7C). Furthermore, the Nar group revealed a substantial upregulation of 296 genes and a downregulation of 445 genes in comparison to the OVX group (Fig. S7D).

A GO enrichment analysis was conducted for various groups. As shown in Fig. 7A, the OVX group exhibited the most significant increase in *calmodulin fixation*, and the downward regulation of *caffeine oxidase activity* was more significant than that in the SO group.

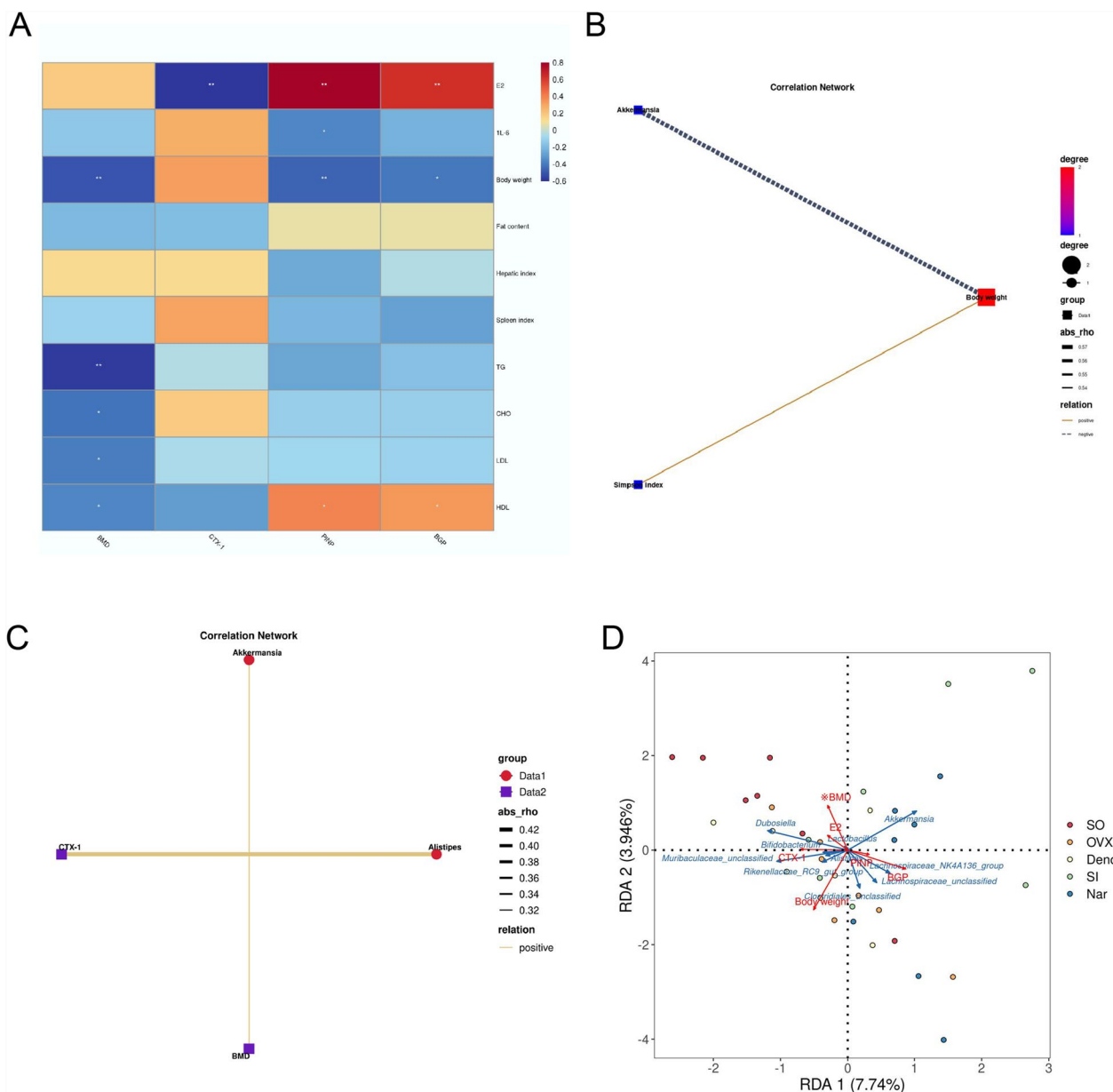


**Fig. 6** Flora analysis and correlation between the intestinal flora and the osteoporosis phenotype. **A** Correlation analysis between bone metabolism and other related indices. **B, C** Correlation analysis between bone-related indices and the intestinal microbiome. **D** Redundancy Analysis (RDA) of the gut microbiome and bone-related indices. All data were mapped and analyzed using R 4.2.1. *n* = 7

Compared with the OVX group, the most altered enrichment in the Deno group was the *inflammatory response*, and the most obvious difference was the shift in the *actin-myosin filaments* (Fig. 7B). In the SI group, *actin filament-based movement* was the most significantly increased, and *monooxygenase activity* was the most significantly decreased relative to that in the OVX group (Fig. 7C). Compared with that in the OVX group, the gene whose expression was significantly

upregulated in the Nar group was *blood circulation*, and the gene whose expression was significantly downregulated was *short-chain fatty acid catabolism* (Fig. 7D).

As shown in Fig. 7E, we conducted an analysis of the 30 genes exhibiting the highest levels of expression within each group. Among them, the genes *Cyp2c55*, *Sst*, *Fabp4*, *Pla2g4c*, *Cyp2c65*, and *Cfd* were significantly better regulated in the OVX group ( $P < 0.0001$ ), while

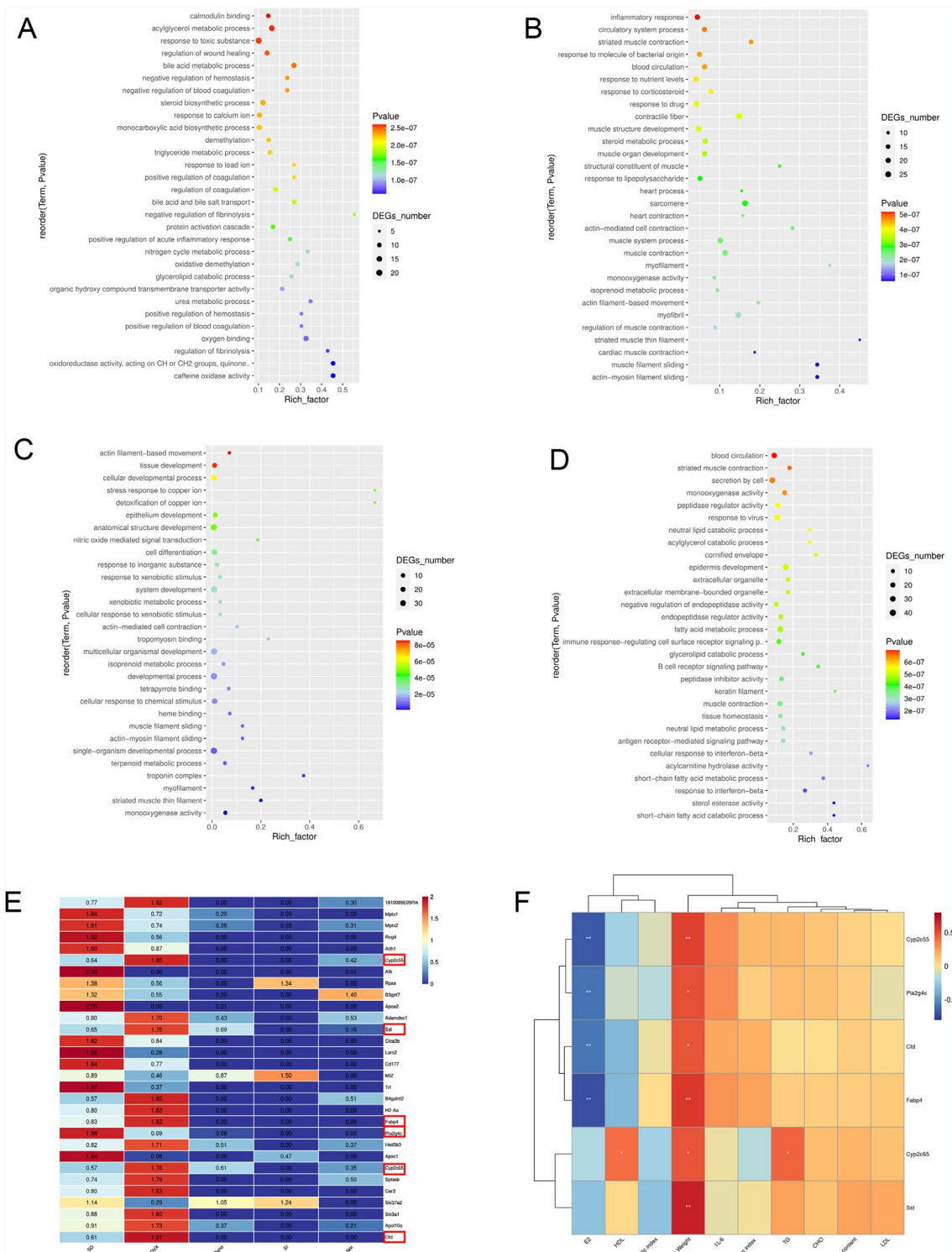


**Fig. 7** Changes in intestinal gene expression. **A–D** Gene Ontology (GO) enrichment of differentially expressed genes among the study groups. **A**—OVX (Ovariectomy) vs. SO (Sham Operation); **B**—Deno (Denosumab) vs. OVX; **C**—Si (Isoflavone) vs. OVX; **D**—Nar (Naringin) vs. OVX. **E** Heatmap of significantly differentially expressed genes in the different study groups. **F** Correlation analysis between target genes and associated indicators. The red box in panel 'E' indicates genes related to our research. All the data were mapped and analyzed using R 4.2.1.  $n = 5$

they were markedly significantly underregulated in the Deno, SI, and Nar groups ( $P < 0.0001$ ).

As shown in Fig. 7E, a correlation analysis was conducted to examine the relationships between target genes and associated indicators. The genes *Cyp2c55*, *Pla2g4c*, *Cfd*, *Fabp4*, *Cyp2c65*, and *Sst* were positively correlated with body weight, TG, CHO, fat content, LDL, and IL-6 and negatively correlated with E2. Notably, body weight showed a strong correlation with these six genes ( $P < 0.05$ ). Additionally, E2 was significantly related to *Cyp2c55*, *Pla2g4c*, *Cfd*, and *Fabp4* ( $P < 0.05$ ). Furthermore, HDL and TG were significantly associated with *Cyp2c65* ( $P < 0.05$ ).

**Effects of phytohormones and denosumab on the ileum ultrastructure and intestinal segment length**

The length of the intestinal segments was found to be significantly longer in the SI and Nar groups compared to the SO and Deno groups, particularly in the ileum and jejunum ( $P < 0.05$ ; Fig. 8A, B). No significant differences in the lengths of the colon or cecum were observed among the study groups. Hence, SI and Nar increased the

intestinal segment length more significantly than SO and Deno did, especially the ileum and jejunum lengths.

At  $\times 7,000$  magnification, the density of ileum villi in the OVX group was significantly lower compared to the SO, Deno, SI, and Nar groups (Fig. 8C). At  $\times 1500$  magnification, the gaps at the tight junctions in the OVX group were notably wider than those observed in the SO group. In contrast, the tight junctions in the SI and Nar groups were significantly narrower and more compact than those in the OVX group, while the gaps in the Deno group were similar to those in the OVX group. Hence, SI and Nar confer protective effects on the ultrastructure of the ileum, whereas Deno does not have similar effects.

**Discussion**

In this study, we conducted a comparative analysis of the effects of SI and Nar in relation to Deno on postmenopausal mice with osteoporosis, while also elucidating a mechanism linked to the bone-intestinal axis. Our findings demonstrated that SI, Nar, and Deno significantly increased hormone levels and enhanced the overall health of osteoporotic mice. SI and Nar

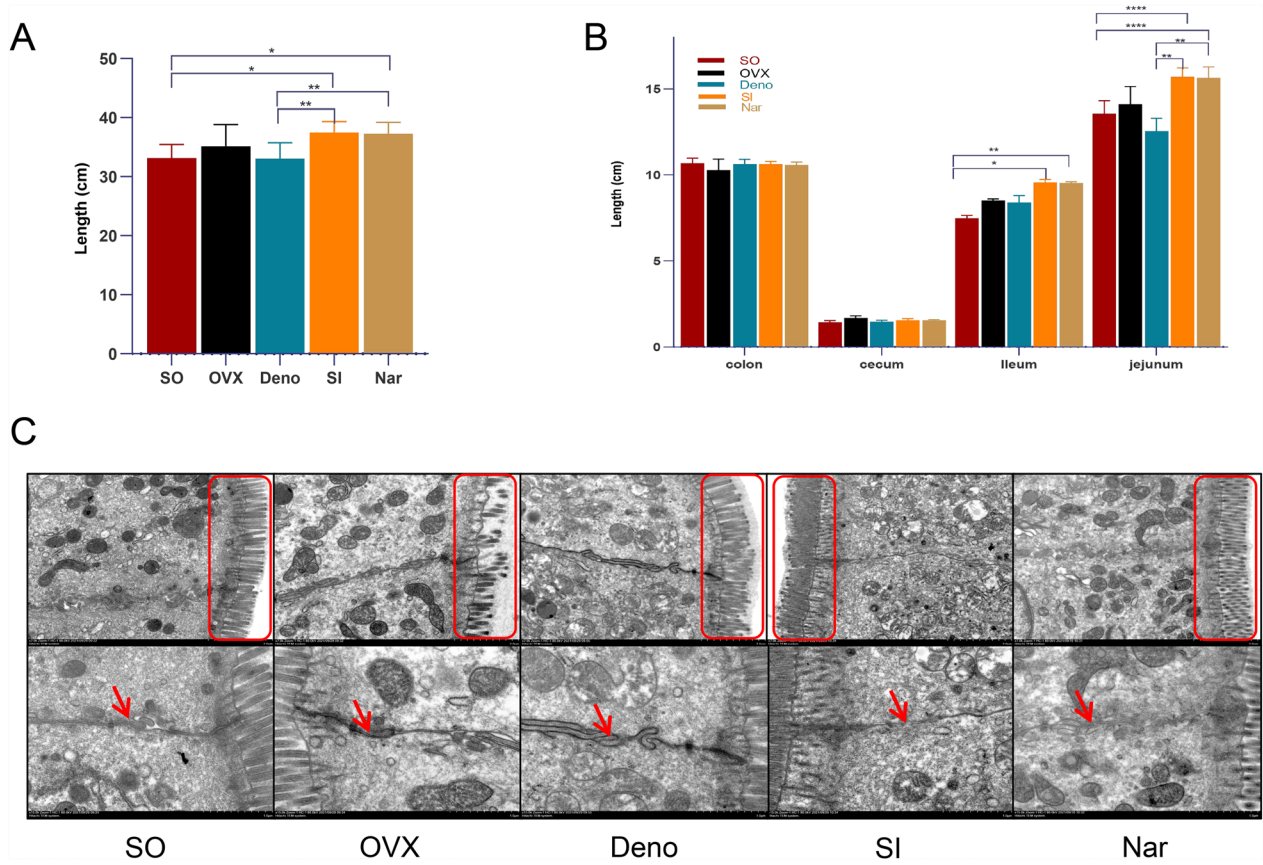


**Fig. 8** Gut-related indicators. **A** Total length of intestine, **B** Intestinal segment length. **C** Ileal ultrastructure. Tight junctions are indicated with red arrows, whereas the red box indicates the villi. All the data are expressed as mean  $\pm$  SD.  $n = 7$ ,  $*P < 0.05$ ,  $**P < 0.01$ ,  $***P < 0.001$ , and  $****P < 0.0001$

showed comparable therapeutic effects to Deno with respect to serum estradiol levels and the expression of osteoporosis biomarkers, including BMD, osteoclast count, CTX-1, BGP, and PINP. Above all, based on the well-established imaging, pathology, and blood markers of bone metabolism [31, 32], our study suggest that, similar to the first-line drug Deno, SI and Nar can effectively replenish hormone levels and improve bone health in postmenopausal osteoporotic mice.

Deno, SI, and Nar promote bone health by regulating body weight, fat mass index, blood lipid levels, and inflammatory markers. In the present study, SI and Nar reduced the weight gain associated with ovariectomy, which was accompanied by a decrease in the abdominal fat content, while simultaneously enhancing blood lipid profiles and reducing inflammatory factors. It is important to note that weight gain in isolation does not inherently lead to a reduction in BMD; however, weight gain accompanied by increased fat mass and hyperlipidemia may contribute to diminished BMD [33]. The established relationship between blood lipids and inflammation is well-documented, yet the connection between blood lipids and bone health remains contentious [34, 35]. Dyslipidemia, particularly alterations in CHO, TG, and LDL contents, has been shown to mediate the systemic inflammatory response, leading to reduced bone mass and elevated risk of fractures [34, 35]. Furthermore, fat accumulation can disrupt bone homeostasis and increase fracture risk, while decreased blood lipids can regulate osteoclast activity [36]. Interestingly, Nar exhibited a better ameliorative effect than SI did in increasing HDL. However, the existing literature on the association between HDL and BMD is ambiguous, with some studies reporting both negative and positive correlations [37, 38]. In the present study, HDL was negatively correlated with BMD but significantly positively correlated with PINP and BGP, suggesting that an increase in HDL may have beneficial effects on bone metabolism. In summary, these findings indicate that SI and Nar promote bone health by reducing body weight, which is associated with hyperlipidemia and high fat content.

In this study, compared with the OVX group, there was an increase in the proportions of *Muribaculaceae\_unclassified*, *Lactobacillus*, *Bifidobacterium*, and *Dubosiella* in the Deno group, alongside a decrease in *Alistipes*. *Muribaculaceae*, *Lactobacillus*, and *Dubosiella* have been shown to promote bone health in mice with osteoporosis [39–42]. In ovariectomized rats, bone loss was improved by an increase in *Bifidobacterium* and a decrease in *Alistipes* [43]. Moreover, the reduction in *Alistipes* decreased the content of CTX-1, a biomarker indicative of bone resorption.

Furthermore, the increased abundances of *Akkermansia*, *Muribaculaceae*, *Bifidobacterium*, and *Dubosiella* have been linked to elevated levels of acetic acid [42, 44–46]. Given the requirement for Deno to be administered subcutaneously, we hypothesize that Deno may not exert a direct influence on the intestinal microbiota. Nonetheless, the observed alterations in certain bacterial populations suggest that the potential role of Deno in modulating intestinal flora, particularly following prolonged administration or through alternative routes of administration, warrants further investigation.

Different with the Deno, research has demonstrated that SI and Nar can reverse the imbalance of the gut microbiota associated with conditions prevalent among women, including estrogen deficiency, obesity, and polycystic ovary syndrome. These interventions have been shown to enhance the abundance of beneficial bacterial populations while diminishing the prevalence of pathogenic bacteria [24, 25, 47–49]. According to the bacterial distribution, we found that the bacterial clusters formed in the Nar and SI groups exhibited significant differences compared to those in the other groups. Notably, *Akkermansia* was significantly enriched in both the SI and Nar groups.

*Akkermansia* shows great potential in the treatment strategy of osteoporosis [50]. This bacterium is a crucial constituent of the gut microbiota and is the only species identified within the phylum Verrucomicrobia in the mammalian intestine [51]. The altered gut microbiota composition in ovariectomized mice following the intestinal microbial transplantation is associated with an increase in the abundance of *Akkermansia* [52]. A research investigation examining the association between osteoporosis and gut microbiota within the population of Henan Province, China, revealed that *Akkermansia* exhibited a negative correlation with markers indicative of bone resorption, while demonstrating a positive correlation with markers associated with bone formation and 25-OH-D3 [53]. Research indicates that the replenishment of *Akkermansia* can rectify the disruption of bone metabolism resulting from ovariectomy. Extracellular vesicles secreted by *Akkermansia* have the capacity to infiltrate bone tissue, where they directly facilitate the osteogenic differentiation of bone marrow mesenchymal stem cells while simultaneously inhibiting the differentiation of osteoclasts from bone marrow mononuclear cells/macrophages. This dual action promotes bone formation and suppresses osteoclastic resorption, thereby mitigating the deterioration of bone microstructure and the reduction in bone mass and strength associated with estrogen deficiency [54].

Studies have shown that *Akkermansia* can enhance bone formation and facilitate fracture healing by

decreasing intestinal permeability and inflammation [55] *Akkermansia* has been demonstrated to lower levels of systemic inflammation [56–58]. Especially, *Akkermansia* can alleviate periodontal inflammation and periodontal bone destruction in mice [59]. The proportion of acetic acid was found to be increased in the Deno, SI, and Nar groups in our study. The increased abundance of *Akkermansia* is reportedly associated with the increase of acetic acid [44]. Acetate positively influences host energy metabolism by stimulating the secretion of intestinal hormones, reducing systemic lipolysis, lowering systemic levels of pro-inflammatory cytokines, and increasing energy expenditure and fat oxidation [60, 61]. In a study conducted on the colon of goats, Tao et al. observed that the widening of gaps in tight junctions compromises the integrity of colonic epithelial tissue [62]. *Akkermansia* has been shown to facilitate the regeneration of intestinal epithelial cells, improve the enterocyte apoptosis, and maintain intestinal homeostasis [57, 63]. Atrophy of the intestinal villi and muscle layer may lead to intestinal obstruction, whereas increased density of intestinal villi enhances intestinal peristalsis and promotes colon health [64]. All treatments administered post-ovariectomy contributed to the amelioration of villus atrophy and the expansion of tight junction gaps within the intestinal lining. Collectively, these findings suggest that *Akkermansia* promotes bone health directly or indirectly via metabolism, body weight, lipid profiles, and inflammatory processes. Additionally, its role in providing intestinal protection and elevating acetic acid levels may facilitate improved intestinal motility in castrated mice, leading to weight reduction, which is advantageous for bone health.

The expression of intestinal genes exhibited comparability following treatment with soy isoflavone, naringin, or Deno. Notably, the Nar intervention resulted in a more pronounced upregulation or downregulation of genes in ovariectomized mice compared to Deno or soy isoflavone. The increase in calmodulin binding after ovariectomy represents an increase in the intracellular calcium ion concentration, which could initiate various physiological mechanisms, such as muscle contraction, neurotransmitter release, hormone secretion, and apoptosis [65]. The reduction of *Fibroxylin* in the OVX group can help stimulate fibroblasts, improve muscle function, mitigate fall risk, and thus improve bone mass [66]. In the Deno group, genes associated with the inflammatory response were upregulated, while those related to actin-myosin filament sliding were downregulated. A study on kidney disease indicated that actin endocytosis was enriched among downregulated proteins in affected patients, whereas proteins associated with inflammatory diseases were enriched among

upregulated proteins [67]. Furthermore, genes associated with actin filament-based movement were upregulated in the SI group, potentially correlating with the level of E2 [68]. The downregulation of monooxygenase expression in the SI group indicated increased anti-inflammatory and antioxidative activities [69]. In contrast, genes related to the SCFA catabolic process were downregulated in the Nar group. The reduced enrichment of SCFAs did not significantly alter the total acid content but resulted in an increased proportion of acetic acid. Given the extensive number of genes associated with GO enrichment, providing a precise explanation of the effects of GO enrichment poses challenges. Consequently, we proceeded to analyze the genes with high expression levels.

In terms of the genes that were differentially expressed, *Cyp2c55* and *Cyp2c65*, the main target genes of the PXR-dependent biological pathways involved in microbiota depletion, were increased in ovariectomized mice but decreased following Deno, SI, and Nar replacement, which was consistent with the serum E2 levels [70]. The deletion of *Sst* was found to modify the structure of the bacterial community, elevate potassium ion concentrations, decrease sodium ion concentrations, and contribute to the maintenance of tissue stability [71]. These results were corroborated by transmission electron microscopy analyses of colonic tissues from ovariectomized mice. Moreover, *Sst* has been shown to locally inhibit the proliferation and differentiation of chondrocytes and bone osteoprogenitor cells. *FABP4* regulates the development and metabolism of inflammation, resists atherosclerosis, and improves insulin sensitivity [72]. The gene *Pla2g4C* has been positively associated with hepatitis and is implicated in the accumulation of hepatic fat, which correlates with an increase in inflammatory factors following ovariectomy and their subsequent reduction post-intervention [73]. Finally, *CFD* is a serine protein kinase known to stimulate adipose tissue secretion, aligning with observed changes in blood lipid levels, body weight, and visceral fat index [74]. Based on these findings, we propose that intestinal gene expression in ovariectomized mice remains relatively consistent following treatment with SI, Nar, or Deno. Furthermore, the effects on the gut in ovariectomized mice are likely related to the regulation of gut E2, lipid metabolism, and inflammation-related genes.

Phytohormones demonstrate a dose-dependent response in the management of various diseases. In women aged 65 and older, both low doses ( $\leq 80$  mg/d) and high doses ( $> 80$  mg/d) of SI were associated with a decrease in TG levels; however, only high doses were found to elevate HDL levels [75]. A separate meta-analysis

indicated that SI administered at doses below 90 mg/d was more effective in enhancing bone markers, including osteoprotegerin, pyridinoline, and C-telopeptides, in overweight and obese populations [76]. However, SI at doses exceeding 84 mg/d was shown to significantly lower IL-6 levels [77]. Furthermore, in female Golden Syrian hamsters, the cholesterol-lowering effects of isoflavones were amplified with increasing dosages. Similarly, naringenin exhibited a dose-dependent influence on glucose and lipid metabolism in diabetic patients [78, 79] and demonstrated inhibitory effects on tumor development. This study did not incorporate dose-gradient experiments, thus raising the question of whether a dose–response relationship exists for these two phytohormones in the treatment of osteoporosis in women, which warrants further exploration. Additionally, the regulatory effects of prebiotics on gut microbiota are also characterized by dose dependency [80, 81]. The current study leaves the potential effects of varying doses of SI and Nar on gut microbiota unclear, highlighting the necessity for further refinement and in-depth investigation in this area.

### Conclusions and limitations

Our findings indicate that, similar to the first-line medication Deno, SI and Nar can effectively enhance hormone levels and promote bone and intestinal health in postmenopausal osteoporosis mice, which may be mediated by gut microbiota. Both plant hormones significantly increased the abundance of *Akkermansia* bacteria in the mouse gut. *Akkermansia* has been shown to improve the loss of bone mass and strength associated with estrogen shortage by blocking the formation of osteoclasts from bone marrow monocytes/macrophages and directly promoting osteogenic differentiation of bone marrow mesenchymal stem cells through extracellular vesicles. In addition, *Akkermansia* can also promote intestinal and bone health by reducing systemic inflammation and regulating lipid metabolism. The alterations in intestinal gene expression confirm this, as Deno, SI, and Nar all reduced the elevated levels of lipid metabolism (*Cyp2c55*, *Cyp2c65*, *Pla2g4C* *FABP4*) and inflammation-related genes (*Pla2g4C*, *FABP4*, *CFD*), as well as bone remodeling-related genes (*Sst*) in the OVX group. It is noteworthy that Deno may not be able to directly modulate the gut microbiota due to the mode of administration. However, long-term administration and different modes of administration warrant further investigation. Furthermore, this research has yet to determine a dose–response relationship, and further investigation is necessary

to elucidate the regulatory effects of varying doses of SI and Nar on postmenopausal osteoporosis, and it is important to examine whether the modulation of the gut microbiota by phytohormones differs across various dosages.

### Abbreviations

SO	Sham-operated
OVX	Ovariectomized
Deno	Denosumab
SI	Soybean isoflavone
Nar	Naringenin
E2	Estradiol
IL-6	Interleukin-6
CTX-1	C-terminal telopeptides of type I collagen
BGP	Bone glycoprotein
PINP	Procollagen I N-terminal propeptide
TG	Triglyceride
CHO	Total cholesterol
HDL-C	High-density lipoprotein cholesterol
LDL-C	Low-density lipoprotein cholesterol
ELISA	Enzyme-linked immunosorbent assay
BMD	Bone mineral density
CT	Computed tomography
SCFAs	Short-chain fatty acids
BW	Body weight
PCoA	Principal coordinates analysis
PCA	Principal component analysis
NMDS	Nonmetric multidimensional scaling
RDA	Redundancy analysis
LDA	Linear discriminant analysis

### Supplementary Information

The online version contains supplementary material available at <https://doi.org/10.1186/s12967-025-06426-1>.

Supplementary material 1.

### Acknowledgements

We would like to thank the "Active Health and Aging Science and Technology Response" of the National Key R & Program of China (Grant No. 2022YFC2010101) and the "Pioneer" and "Leading Goose" R&D Program of Zhejiang (Grant No. 2022C03138).

### Author contributions

JL and XH: funding acquisition and project administration. JL, XH, ZZ, YD, LZ, Li Li, XL, XW, HS: investigation. JL, XH, LZ, XL, XW: Methodology. ZZ: experimentation, data analysis, writing the original draft, reviewing, and editing. JL, XH, XL: reviewing, and editing. All the authors have contributed to the manuscript and approved the submitted version.

### Funding

This study was supported by the "Active Health and Aging Science and Technology Response" of the National Key R & Program of China (Grant No. 2022YFC2010101) and the "Pioneer" and "Leading Goose" R&D Program of Zhejiang (Grant No. 2022C03138).

### Availability of data and materials

The datasets presented in this study can be found in the BioProject PRJNA970989 and PIJNA825110 in the NCBI GenBank database.

## Declarations

### Ethics approval and consent to participate

This study was funded by the Ethics Committee of Zhejiang Province, and the animal experiments were conducted at the Zhejiang Academy of Agricultural Sciences (License No. 2021ZAASLA50).

### Consent for publication

Jinjun Li, Zhiqih Zhao, Yixuan Deng, Lili, Liying Zhu, XinWang, Haibiao Sun, Xiaoqiong Li, and Xiaoqiang Han confirm that we have reviewed and agree with the contents of the submitted manuscript.

### Competing interests

All the authors declare that they have no conflicts of interest.

### Author details

<sup>1</sup>State Key Laboratory for Quality and Safety of Agro-Products & Institute of Food Sciences, Zhejiang Academy of Agricultural Sciences, Hangzhou 310021, China. <sup>2</sup>Department of Orthopedics, The First Hospital of Shanxi Medical University, Taiyuan 030000, China. <sup>3</sup>School of Medicine, Wenzhou Medical University, Chashan University Town, Wenzhou 325035, Zhejiang, People's Republic of China. <sup>4</sup>Clinical Medical College, Hangzhou Normal University, Hangzhou 30021, China.

Received: 9 September 2024 Accepted: 25 March 2025

Published online: 09 April 2025

## References

1. Wa P. Consensus development conference: diagnosis, prophylaxis, and treatment of osteoporosis. *Am J Med.* 1993;94:646–50.
2. Słupski W, Jawień P, Nowak B. Botanicals in postmenopausal osteoporosis. *Nutrients.* 2021;13:1609.
3. Bone HG, Wagman RB, Brandi ML, Brown JP, Chapurlat R, Cummings SR, Czerwiński E, Fahrleitner-Pammer A, Kendler DL, Lippuner K, et al. 10 years of denosumab treatment in postmenopausal women with osteoporosis: results from the phase 3 randomised FREEDOM trial and open-label extension. *Lancet Diabetes Endocrinol.* 2017;5:513–23.
4. Eastell R, O'Neill TW, Hofbauer LC, Langdahl B, Reid IR, Gold DT, Cummings SR. Postmenopausal osteoporosis. *Nat Rev Dis Primers.* 2016;2:16069.
5. Hamm AK, Manter DK, Kirkwood JS, Wolfe LM, Cox-York K, Weir TL. The effect of Hops (*Humulus lupulus* L.) extract supplementation on weight gain, adiposity and intestinal function in ovariectomized mice. *Nutrients.* 2019;11:3004.
6. Nakano M, Omae N, Tsuda K. Inter-organismal phytohormone networks in plant-microbe interactions. *Curr Opin Plant Biol.* 2022;68: 102258.
7. Lagari VS, Levis S. Phytoestrogens in the prevention of postmenopausal bone loss. *J Clin Densitom.* 2013;16:445–9.
8. Ramesh P, Jagadeesan R, Sekaran S, Dhanasekaran A, Vimalraj S. Flavonoids: classification, function, and molecular mechanisms involved in bone remodelling. *Front Endocrinol.* 2021;12: 779638.
9. Bellavia D, Dimarco E, Costa V, Carina V, De Luca A, Raimondi L, Fini M, Gentile C, Caradonna F, Giavaresi G. Flavonoids in bone erosive diseases: perspectives in osteoporosis treatment. *Trends Endocrinol Metab.* 2021;32:76–94.
10. Liu ZM, Ho SC, Woo J, Chen YM, Wong C. Randomized controlled trial of whole soy and isoflavone daidzein on menopausal symptoms in equol-producing Chinese postmenopausal women. *Menopause.* 2014;21:653–60.
11. Adlercreutz H, Mazur W. Phyto-estrogens and Western diseases. *Ann Med.* 1997;29:95–120.
12. Wang X, Chen B, Fang X, Zhong Q, Liao Z, Wang J, Wu X, Ma Y, Li P, Feng X, Wang L. Soy isoflavone-specific biotransformation product S-equol in the colon: physiological functions, transformation mechanisms, and metabolic regulatory pathways. *Crit Rev Food Sci Nutr.* 2022;64:1–29.
13. George KS, Muñoz J, Akhavan NS, Foley EM, Siebert SC, Tenenbaum G, Khalil DA, Chai SC, Arjmandi BH. Is soy protein effective in reducing cholesterol and improving bone health? *Food Funct.* 2020;11:544–51.
14. Pohjanvirta R, Nasri A. The potent phytoestrogen 8-prenylnaringenin: a friend or a foe? *Int J Mol Sci.* 2022;23:3168.
15. Kaczmarczyk-Sedlak I, Wojnar W, Zych M, Ozimina-Kamińska E, Bońka A. Effect of dietary flavonoid naringenin on bones in rats with ovariectomy-induced osteoporosis. *Acta Pol Pharm.* 2016;73:1073–81.
16. Habauzit V, Verny MA, Milenkovic D, Barber-Chamoux N, Mazur A, Dubray C, Morand C. Flavonones protect from arterial stiffness in postmenopausal women consuming grapefruit juice for 6 mo: a randomized, controlled, crossover trial. *Am J Clin Nutr.* 2015;102:66–74.
17. Namkhah Z, Naeini F, Mahdi Rezayat S, Mehdi Y, Mansouri S, Javad Hosseinzadeh-Attar M. Does naringenin supplementation improve lipid profile, severity of hepatic steatosis and probability of liver fibrosis in overweight/obese patients with NAFLD? A randomised, double-blind, placebo-controlled, clinical trial. *Int J Clin Pract.* 2021;75: e14852.
18. Tu Y, Yang R, Xu X, Zhou X. The microbiota-gut-bone axis and bone health. *J Leukoc Biol.* 2021;110:525–37.
19. Castaneda M, Smith KM, Nixon JC, Hernandez CJ, Rowan S. Alterations to the gut microbiome impair bone tissue strength in aged mice. *Bone Rep.* 2021;14: 101065.
20. Heiskanen JT, Kröger H, Pääkkönen M, Parviainen MT, Lamberg-Allardt C, Alhava E. Bone mineral metabolism after total gastrectomy. *Bone.* 2001;28:123–7.
21. Yan J, Herzog JW, Tsang K, Brennan CA, Bower MA, Garrett WS, Sartor BR, Aliprantis AO, Charles JF. Gut microbiota induce IGF-1 and promote bone formation and growth. *Proc Natl Acad Sci USA.* 2016;113:E7554–e7563.
22. Ratajczak AE, Rychter AM, Zawada A, Dobrowolska A, Krela-Kaźmierczak I. Do only calcium and vitamin D matter? Micronutrients in the diet of inflammatory bowel diseases patients and the risk of osteoporosis. *Nutrients.* 2021;13:525.
23. Stevens Y, Rymenant EV, Grootaert C, Camp JV, Possemiers S, Masclee A, Jonkers D. The intestinal fate of citrus flavanones and their effects on gastrointestinal health. *Nutrients.* 2019;11:1464.
24. Leonard LM, Choi MS, Cross TL. Maximizing the estrogenic potential of soy isoflavones through the gut microbiome: implication for cardiometabolic health in postmenopausal women. *Nutrients.* 2022;14:553.
25. Wu YY, Gou W, Yan Y, Liu CY, Yang Y, Chen D, Xie K, Jiang Z, Fu Y, Zhu HL, et al. Gut microbiota and acylcarnitine metabolites connect the beneficial association between equol and adiposity in adults: a prospective cohort study. *Am J Clin Nutr.* 2022;116:1831–41.
26. Komori T. Animal models for osteoporosis. *Eur J Pharmacol.* 2015;759:287–94.
27. Zheng L, Zhuang Z, Li Y, Shi T, Fu K, Yan W, Zhang L, Wang P, Li L, Jiang Q. Bone targeting antioxidative nano-iron oxide for treating postmenopausal osteoporosis. *Bioact Mater.* 2022;14:250–61.
28. Liu X, He C, Koyama T. D-Pinitol ameliorated osteoporosis via elevating D-chiro-inositol level in ovariectomized mice. *J Nutr Sci Vitaminol (Tokyo).* 2023;69:220–8.
29. Liu J, Ding S, Yang L, Zhao X, Ren R, Wang Y, Su C, Chen J, Ma X. Integration of pharmacodynamics and metabolomics reveals the therapeutic effects of 6-acetylacteoside on ovariectomy-induced osteoporosis mice. *Phytomedicine.* 2022;106: 154399.
30. Pi X, Hua H, Wu Q, Wang X, Wang X, Li J. Effects of different feeding methods on the structure, metabolism, and gas production of infant and toddler intestinal flora and their mechanisms. *Nutrients.* 2022;14:1568.
31. Camacho PM, Petak SM, Binkley N, Diab DL, Eldeiry LS, Farooki A, Harris ST, Hurlley DL, Kelly J, Lewiecki EM, et al. American association of clinical endocrinologists/American college of endocrinology clinical practice guidelines for the diagnosis and treatment of postmenopausal osteoporosis-2020 update. *Endocr Pract.* 2020;26:1–46.
32. Aibar-Almazán A, Voltés-Martínez A, Castellote-Caballero Y, Afanador-Restrepo DF, Carcelén-Fraile MDC, López-Ruiz E. Current status of the diagnosis and management of osteoporosis. *Int J Mol Sci.* 2022;23:9465.
33. López-Peralta S, Romero-Velarde E, Vásquez-Garibay EM, González-Hita M, Robles-Robles LC, Ruiz-González FJ, Pérez-Romero MA. Bone mineral density and body composition in normal weight, overweight and obese children. *BMC Pediatr.* 2022;22:249.
34. Martín-González C, González-Reimers E, Quintero-Platt G, Cabrera-García P, Romero-Acevedo L, Gómez-Rodríguez M, Rodríguez Gaspar

- M, Martínez-Martínez D, Santolaria-Fernández F. Lipid profile and bone mineral density in heavy alcoholics. *Clin Nutr.* 2018;37:2137–43.
35. Anagnostis P, Florentin M, Livadas S, Lambrinouadaki I, Goulis DG. Bone health in patients with dyslipidemias: an underestimated aspect. *Int J Mol Sci.* 2022;23:1639.
  36. Kim H, Oh B, Park-Min KH. Regulation of osteoclast differentiation and activity by lipid metabolism. *Cells.* 2021;10:89.
  37. Tang Y, Wang S, Yi Q, Xia Y, Geng B. High-density lipoprotein cholesterol is negatively correlated with bone mineral density and has potential predictive value for bone loss. *Lipids Health Dis.* 2021;20:75.
  38. Xie R, Huang X, Liu Q, Liu M. Positive association between high-density lipoprotein cholesterol and bone mineral density in U.S. adults: the NHANES 2011–2018. *J Orthop Surg Res.* 2022;17:92.
  39. Li P, Ji B, Luo H, Sundh D, Lorentzon M, Nielsen J. One-year supplementation with *Lactobacillus reuteri* ATCC PTA 6475 counteracts a degradation of gut microbiota in older women with low bone mineral density. *NPJ Biofilms Microbiomes.* 2022;8:84.
  40. Kwon Y, Park C, Lee J, Park DH, Jeong S, Yun CH, Park OJ, Han SH. Regulation of bone cell differentiation and activation by microbe-associated molecular patterns. *Int J Mol Sci.* 2021;22:5805.
  41. Zhou J, Wang R, Zhao R, Guo X, Gou P, Bai H, Lei P, Xue Y. Intermittent parathyroid hormone alters gut microbiota in ovariectomized osteoporotic rats. *Orthop Surg.* 2022;14:2330–8.
  42. Tonucci LB, Olbrich Dos Santos KM, Licursi de Oliveira L, Rocha Ribeiro SM, Duarte Martino HS. Clinical application of probiotics in type 2 diabetes mellitus: a randomized, double-blind, placebo-controlled study. *Clin Nutr.* 2017;36:85–92.
  43. Zhu Y, Liu S, Mei F, Zhao M, Xia G, Shen X. *Tilapia nilotica* head lipids improved bone loss by regulating inflammation and serum metabolism through gut microbiota in ovariectomized rats. *Front Nutr.* 2021;8: 792793.
  44. Wang Z, Qin X, Hu D, Huang J, Guo E, Xiao R, Li W, Sun C, Chen G. Akkermansia supplementation reverses the tumor-promoting effect of the fecal microbiota transplantation in ovarian cancer. *Cell Rep.* 2022;41: 111890.
  45. Łagowska K, Drzymala-Czyż S. A low glycemic index, energy-restricted diet but not *Lactobacillus rhamnosus* supplementation changes fecal short-chain fatty acid and serum lipid concentrations in women with overweight or obesity and polycystic ovary syndrome. *Eur Rev Med Pharmacol Sci.* 2022;26:917–26.
  46. Guo Z, Liu Y, Xiang J, Liang X. Mechanochemical preparation of red clover extract/ $\beta$ -cyclodextrin dispersion: enhanced water solubility and activities in alleviating high-fat diet-induced lipid accumulation and gut microbiota dysbiosis in mice. *Food Chem.* 2023;420: 136084.
  47. Wu YX, Yang XY, Han BS, Hu YY, An T, Lv BH, Lian J, Wang TY, Bao XL, Gao L, Jiang GJ. Naringenin regulates gut microbiota and SIRT1/PGC-1 $\alpha$  signaling pathway in rats with letrozole-induced polycystic ovary syndrome. *Biomed Pharmacother.* 2022;153: 113286.
  48. Qin S, Wang Y, Wang S, Ning B, Hual J, Yang H. Gut microbiota in women with gestational diabetes mellitus has potential impact on metabolism in pregnant mice and their offspring. *Front Microbiol.* 2022;13: 870422.
  49. Wang L, Wu X, Ma Y, Li X, Zhang J, Zhao L. Supplementation with soy isoflavones alleviates depression-like behaviour via reshaping the gut microbiota structure. *Food Funct.* 2021;12:4995–5006.
  50. Keshavarz Azizi Raftar S, Hoseini Tavassol Z, Amiri M, Ejtahed HS, Zangeneh M, Sadeghi S, Ashrafiyan F, Kariman A, Khatami S, Siadat SD. Assessment of fecal Akkermansia muciniphila in patients with osteoporosis and osteopenia: a pilot study. *J Diabetes Metab Disord.* 2021;20:279–284.
  51. Becken B, Davey L, Middleton DR, Mueller KD, Sharma A, Holmes ZC, Dallow E, Remick B, Barton GM, David LA, et al. Genotypic and phenotypic diversity among human isolates of akkermansia muciniphila. *MBio.* 2021;12:10–128.
  52. Chevalier C, Kieser S, Çolakoglu M, Hadadi N, Brun J, Rigo D, Suárez-Zamorano N, Špiljar M, Fabbiano S, Busse B, et al. Warmth prevents bone loss through the gut microbiota. *Cell Metab.* 2020;32:575–590. e577.
  53. Qin Q, Yan S, Yang Y, Chen J, Yan H, Li T, Gao X, Wang Y, Li A, Wang S, Ding S. The Relationship Between Osteoporosis and Intestinal Microbes in the Henan Province of China. *Front Cell Dev Biol.* 2021;9:752990.
  54. Liu JH, Chen CY, Liu ZZ, Luo ZW, Rao SS, Jin L, Wan TF, Yue T, Tan YJ, Yin H, et al. Extracellular vesicles from child gut microbiota enter into bone to preserve bone mass and strength. *Adv Sci (Weinh).* 2021;8:2004831.
  55. Liu JH, Yue T, Luo ZW, Cao J, Yan ZQ, Jin L, Wan TF, Shuai CJ, Wang ZG, Zhou Y, et al. Akkermansia muciniphila promotes type H vessel formation and bone fracture healing by reducing gut permeability and inflammation. *Dis Model Mech.* 2020;13.
  56. Qu S, Fan L, Qi Y, Xu C, Hu Y, Chen S, Liu W, Liu W, Si J. Akkermansia muciniphila alleviates dextran sulfate sodium (DSS)-induced acute colitis by NLRP3 activation. *Microbiol Spectr.* 2021;9: e0073021.
  57. Rao Y, Kuang Z, Li C, Guo S, Xu Y, Zhao D, Hu Y, Song B, Jiang Z, Ge Z, et al. Gut Akkermansia muciniphila ameliorates metabolic dysfunction-associated fatty liver disease by regulating the metabolism of L-aspartate via gut-liver axis. *Gut Microbes.* 2021;13:1–19.
  58. Kobylak N, Falalyeyeva T, Kyriachenko Y, Tseyslyer Y, Kovalchuk O, Hadilija O, Esлами M, Yousefi B, Abenavoli L, Fagoonee S, Pellicano R. Akkermansia muciniphila as a novel powerful bacterial player in the treatment of metabolic disorders. *Minerva Endocrinol.* 2022;47:242–52.
  59. Huck O, Mulhall H, Rubin G, Kizelnik Z, Iyer R, Perpich JD, Haque N, Cani PD, de Vos WM, Amar S. Akkermansia muciniphila reduces Porphyromonas gingivalis-induced inflammation and periodontal bone destruction. *J Clin Periodontol.* 2020;47:202–12.
  60. Hernández MAG, Canfora EE, Jocken JWE, Blaak EE. The short-chain fatty acid acetate in body weight control and insulin sensitivity. *Nutrients.* 2019;11.
  61. Koh A, De Vadder F, Kovatcheva-Datchary P, Bäckhed F. From dietary fiber to host physiology: short-chain fatty acids as key bacterial metabolites. *Cell.* 2016;165:1332–45.
  62. Tao S, Duanmu Y, Dong H, Tian J, Ni Y, Zhao R. A high-concentrate diet induced colonic epithelial barrier disruption is associated with the activating of cell apoptosis in lactating goats. *BMC Vet Res.* 2014;10:235.
  63. Kim S, Shin YC, Kim TY, Kim Y, Lee YS, Lee SH, Kim MN, Eunju O, Kim KS, Kweon MN. Mucin degrader Akkermansia muciniphila accelerates intestinal stem cell-mediated epithelial development. *Gut Microbes.* 2021;13:1–20.
  64. Garfinkle R, Trabulsi N, Morin N, Phang T, Liberman S, Feldman L, Fried G, Boutros M. Study protocol evaluating the use of bowel stimulation before loop ileostomy closure to reduce postoperative ileus: a multicenter randomized controlled trial. *Colorectal Dis.* 2017;19:1024–9.
  65. Wu X, Hong L. Calmodulin interactions with voltage-gated sodium channels. *Int J Mol Sci.* 2021;22:9798.
  66. Yong EL, Logan S. Menopausal osteoporosis: screening, prevention and treatment. *Singapore Med J.* 2021;62:159–66.
  67. Stokman MF, Bijnscorp IV, Schelfhorst T, Pham TV, Piersma SR, Knol JC, Giles RH, Bongers E, Knoers N, Lillien MR, et al. Changes in the urinary extracellular vesicle proteome are associated with nephronophthisis-related ciliopathies. *J Proteomics.* 2019;192:27–36.
  68. Mehta D, Rex-Haffner M, Søndergaard HB, Pinborg A, Binder EB, Frokjaer VG. Genome-wide gene expression in a pharmacological hormonal transition model and its relation to depressive symptoms. *Acta Psychiatr Scand.* 2019;140:77–84.
  69. Fernando D, Dimelow R, Gorey C, Zhu X, Muya C, Parker C, Wright W, Soleman S, Walsh S, Crause M, et al. Assessment of the safety, pharmacokinetics and pharmacodynamics of GSK3335065, an inhibitor of kynurenine monooxygenase, in a randomised placebo-controlled first-in-human study in healthy volunteers. *Br J Clin Pharmacol.* 2022;88:865–70.
  70. Barretto SA, Lasserre F, Huillet M, Régnier M, Polizzi A, Lippi Y, Fougerat A, Person E, Bruel S, Bétoulières C, et al. The pregnane X receptor drives sexually dimorphic hepatic changes in lipid and xenobiotic metabolism in response to gut microbiota in mice. *Microbiome.* 2021;9:93.
  71. Lian T, Huang Y, Xie X, Huo X, Shahid MQ, Tian L, Lan T, Jin J. Rice SST variation shapes the rhizosphere bacterial community, conferring tolerance to salt stress through regulating soil metabolites. *MSystems.* 2020;5:10–128.
  72. Prentice KJ, Saksi J, Hotamisligil GS. Adipokine FABP4 integrates energy stores and counterregulatory metabolic responses. *J Lipid Res.* 2019;60:734–40.
  73. Su X, Liu S, Zhang X, Lam SM, Hu X, Zhou Y, Chen J, Wang Y, Wu C, Shui G, et al. Requirement of cytosolic phospholipase A2 gamma in lipid droplet formation. *Biochim Biophys Acta Mol Cell Biol Lipids.* 2017;1862:692–705.

74. Villa-Roel N, Ryu K, Gu L, Fernandez Esmerats J, Kang DW, Kumar S, Jo H. Hypoxia inducible factor 1 $\alpha$  inhibitor PX-478 reduces atherosclerosis in mice. *Atherosclerosis*. 2022;344:20–30.
75. Yang S, Zeng Q, Huang X, Liang Z, Hu H. Effect of isoflavones on blood lipid alterations in postmenopausal females: a systematic review and meta-analysis of randomized trials. *Adv Nutr*. 2023;14:1633–1643.
76. Akhlaghi M, Ghasemi Nasab M, Riasatian M, Sadeghi F. Soy isoflavones prevent bone resorption and loss, a systematic review and meta-analysis of randomized controlled trials. *Crit Rev Food Sci Nutr*. 2020;60:2327–2341.
77. Gholami A, Baradaran HR, Hariri M. Can soy isoflavones plus soy protein change serum levels of interleukin-6? A systematic review and meta-analysis of randomized controlled trials. *Phytother Res*. 2021;35:1147–1162.
78. Rotimi SO, Adelani IB, Bankole GE, Rotimi OA. Naringin enhances reverse cholesterol transport in high fat/low streptozocin induced diabetic rats. *Biomed Pharmacother*. 2018;101:430–437.
79. Pari L, Chandramohan R. Modulatory effects of naringin on hepatic key enzymes of carbohydrate metabolism in high-fat diet/low-dose streptozotocin-induced diabetes in rats. *Gen Physiol Biophys*. 2017;36:343–352.
80. Xiao Q, Luo L, Zhu X, Yan Y, Li S, Chen L, Wang X, Zhang J, Liu D, Liu R, Zhong Y. Formononetin alleviates ulcerative colitis via reshaping the balance of M1/M2 macrophage polarization in a gut microbiota-dependent manner. *Phytomedicine*. 2024;135:156153.
81. Liu Y, Zhong X, Lin S, Xu H, Liang X, Wang Y, Xu J, Wang K, Guo X, Wang J, et al. *Limosilactobacillus reuteri* and caffeoylquinic acid synergistically promote adipose browning and ameliorate obesity-associated disorders. *Microbiome*. 2022;10:226.

### **Publisher's Note**

Springer Nature remains neutral with regard to jurisdictional claims in published maps and institutional affiliations.